The Journal of Immunology

RESEARCH ARTICLE | JULY 15 2008

Elucidation of the MD-2/TLR4 Interface Required for Signaling by Lipid IVa[1]

FREE

Catherine Walsh; ... et. al

J Immunol (2008) 181 (2): 1245–1254.
https://doi.org/10.4049/jimmunol.181.2.1245

Elucidation of the MD-2/TLR4 Interface Required for Signaling by Lipid IVa[1]

Catherine Walsh,[2]* Monique Gangloff,[2†] Tom Monie,[†] Tomoko Smyth,* Bin Wei,* Trevelyan J. McKinley,* Duncan Maskell,* Nicholas Gay,[†] and Clare Bryant[3]*

LPS signals through a membrane bound-complex of the lipid binding protein MD-2 and the receptor TLR4. In this study we identify discrete regions in both MD-2 and TLR4 that are required for signaling by lipid IVa, an LPS derivative that is an agonist in horse but an antagonist in humans. We show that changes in the electrostatic surface potential of both MD-2 and TLR4 are required in order that lipid IVa can induce signaling. In MD-2, replacing horse residues 57–66 and 82–89 with the equivalent human residues confers a level of constitutive activity on horse MD-2, suggesting that conformational switching in this protein is likely to be important in ligand-induced activation of MD-2/TLR4. We identify leucine-rich repeat 14 in the C terminus of TLR4 as essential for lipid IVa activation of MD-2/TLR4. Remarkably, we identify a single residue in the glycan-free flank of the horse TLR4 solenoid that confers the ability to signal in response to lipid IVa. These results suggest a mechanism of signaling that involves crosslinking mediated by both MD-2-receptor and receptor-receptor contacts in a model that shows striking similarities to the recently published structure (*Cell* 130: 1071–1082) of the ligand-bound TLR1/2 ectodomain heterodimer. ***The Journal of Immunology,*** **2008, 181: 1245–1254.**

Lipopolysaccharide molecules are complex glycolipids that form the outer layer of the outer membrane of Gram-negative bacteria (1). The lipid A domain of LPS is responsible for cellular activation and consists of a disaccharide to which various substituents, including acyl chains of variable length and number, are attached (2). *Escherichia coli* lipid A is usually hexa-acylated whereas a tetra-acylated lipid A, lipid IVa, is also produced by *E. coli* as an intermediate in the lipid A biosynthetic pathway (2). Lipid IVa was originally identified as an inhibitor at the human LPS receptor and was considered a candidate to be developed for clinical use as an endotoxin antagonist. Lipid A signals to host cells through a transmembrane complex consisting of the lipid-binding protein MD-2 and the type 1 receptor TLR4 (1, 3–5). MD-2 is probably the key player in lipid A recognition whereas TLR4, unlike other TLRs, is thought not to participate directly in lipid A binding (5).

LPS and lipid A are believed to be recognized by MD-2 following transfer from CD14, which does not participate in the signaling complex (6). Contrary to expectations, ligand binding does not significantly alter the overall structure of MD-2 (7, 8), but the ligands used in the crystallographic studies (lipid IVa and eritoran) are antagonists to human MD-2/TLR4, so it remains unclear what happens to MD-2 and TLR4 upon agonist binding and activation. Active ligands such a lipid A (9) presumably induce structural rearrangements that trigger dimerization of TLR4 and initiate signal transduction (7, 10–13). Mutagenesis studies identified amino acids 79–83, 121–124, 125–129 (12), K128, and K132 of human MD-2 as being important in lipid A binding (13), but in the crystal structure of the inactive MD-2-lipid IVa complex, only residues I46, L78, I80, and F121–I124 contact the ligand. The other residues identified by mutagenesis may play an indirect role in formation of the active complex.

It is still unclear whether TLR4 participates directly in ligand binding and discrimination. TLR4 could play a secondary role in ligand binding because residues in MD-2 (C95 and C105), which are important for TLR4 binding (11, 14), are located at the rim of the ligand-binding cavity (8). This is supported by the higher LPS affinity of the TLR4-MD-2 complex compared with MD-2 on its own (15). Other TLRs do recognize ligands directly. For example, lipopeptides are detected by the leucine-rich repeat (LRR)[4] region 9–12 of TLR1/6 (16, 17), and residues D295 and D367 of TLR5 are important for the recognition of bacterial flagellin (16). MD-2 binds to TLR4 on a lateral surface of the TLR4 solenoid near to the N terminus (18). Interestingly, TLR4 single nucleotide polymorphisms (D299G and T399I) in humans are located far away from the N-terminal MD-2 binding site but reduce LPS responsiveness (19, 20). The mechanism for this is unclear, but the mutations could either affect the cooperative binding of LPS or alter the conformational changes that occur during ligand-induced signal transduction.

There are marked differences among mammalian species in the activities of different types of lipid A that behave as agonists or antagonists at the MD-2/TLR4 complex (21–23). Lipid A is an agonist in most species whereas lipid IVa, while being an agonist in the mouse, is an antagonist for human cells (21, 24). This suggests that lipid IVa is able to bind to human TLR4/MD-2 but is

*Department of Veterinary Medicine and †Department of Biochemistry, University of Cambridge, Cambridge, United Kingdom

Received for publication January 11, 2008. Accepted for publication May 5, 2008.

The costs of publication of this article were defrayed in part by the payment of page charges. This article must therefore be hereby marked *advertisement* in accordance with 18 U.S.C. Section 1734 solely to indicate this fact.

[1] C.W. was supported by a Horserace Betting Levy Board Scholarship and N.G. was supported by a Medical Research Council program grant.

[2] C.W. and M.G. contributed equally to this work.

[3] Address correspondence and reprint requests to Dr. Clare Bryant, Department of Veterinary Medicine, University of Cambridge, Madingley Road, Cambridge, CB3 OES, U.K. E-mail address: ceb27@cam.ac.uk

[4] Abbreviations used in this paper: LRR, leucine-rich repeat; EH, chimera in which a human region is engineered into an equine framework; HE, chimera in which an equine region is engineered into a human framework.

unable to induce signal transduction. By using comparative analysis to study lipid IVa interactions with TLR4/MD-2 from different mammalian species, we therefore have a unique opportunity to identify residues exclusively involved in signal transduction and therefore understand how TLR4/MD-2 performs functionally in an agonistic or antagonist complex. In this study we identify sequences in both MD-2 and TLR4 that are required for signaling activity induced by lipid IVa. These results allow us to propose a structural model of TLR4-MD-2 activation that involves both receptor-MD-2 and receptor-receptor interactions.

Materials and Methods

Constructs

TLR4 and CD14 were cloned into pcDNA3 and MD-2 was subcloned into pEFIRES (25). TLR4 and MD2 chimeras were constructed by overlap extension PCR. Point mutations were introduced either by site-directed mutagenesis (QuikChange; Stratagene) or by overlap extension PCR. Mutations were confirmed by sequencing. Western blot analysis and FACS analysis were used to confirm protein expression levels and cell surface expression, respectively. Both horse and human TLR4 show equal surface expression on HEK cells (2.16% horse TLR4 vs 1.29% human TLR4), but there are slight differences in the intracellular levels of TLR4 expression (7.28% for horse TLR4 vs 3.33% for human TLR4). These levels of TLR4 expression are comparable with those seen by others using similar transient transfection techniques (20).

Cloning of cat TLR4, CD14, and MD-2

RNA was extracted from feline whole blood using the QIAamp RNA blood mini kit (Qiagen). Reverse transcription into cDNA and amplification of first-strand cDNA encoding feline TLR4, CD14, and MD-2 was performed by RACE using the GeneRacer kit (Invitrogen). Fragments were cloned into TOPO vector and checked with restriction digests where the sequence was available (from archive traces), followed by sequencing. TLR4 and CD14 were subcloned into pcDNA3 and MD-2 into pEFIRES.

Cell culture and transient transfection

HEK293 cells were maintained in DMEM supplemented with 10% FCS, 2 mM L-glutamine, 100 $U \cdot ml^{-1}$ penicillin, and 100 $\cdot \mu g\ ml^{-1}$ streptomycin. HEK293 cells were transfected as previously described (26). Briefly, cells were seeded at 3×10^4/well in a 96-well plate and transiently transfected 2 days later. Expression vectors containing cDNA encoding TLR4, MD-2, and CD14 (1 ng/well of each), a NF-κB transcription reporter vector encoding firefly luciferase (5 ng/well pNF-κB-luc; Clontech), and a constitutively active reporter vector encoding *Renilla* luciferase (5 ng/well phRG-TK; Promega), together with empty vector to ensure that an optimal amount of DNA was mixed with jetPEI (Polyplus transfection) according to the manufacturer's instructions. After 48 h, cells were stimulated with Kdo_2-lipid A (3-deoxy-D-*manno*-octulosonic acid-lipid A) or lipid IVa (purified as described in Ref. 9; a gift from Prof. C. Raetz, Duke University, Durham, NC) diluted in DMEM supplemented with 0.1% FCS. TNF-α stimulation (1 $ng \cdot ml^{-1}$) was used as a positive control. The cells were washed with PBS and then lysed and luciferase activity was quantified using the Dual luciferase kit (Promega) according to the manufacturer's instructions. Constructs that failed to signal to Kdo_2-lipid A were excluded from this study.

Molecular modeling

MD-2 models were based on the crystal structure of Der P2 mite dust allergen protein (Protein Data Bank code 1KTJ; Ref. 27) and up-dated using the crystal structure of human MD-2 (Protein Data Bank code 2E56; Ref. 8) as a template (28–30). Briefly, the FUGUE program detected the remote homology between MD-2 and the Der P2 proteins by sequence-structure comparison (28). The alignment generated by FUGUE was analyzed using the JOY software (29) and manually refined. The sequence alignment was optimized by iteration of three-dimensional modeling of the protein structures, followed by assessment of the quality of the models. The 8.2 version with built-in energy minimization features of the modeling software MODELLER (30) was used to generate 30 models, including both conserved regions and loops. The quality of the models was analyzed by the VERIFY3D and PROCHECK programs online (nihserver.mbi.ucla.edu/SAVS/). The models with the best geometry were selected for molecular representation.

TLR4 three-dimensional models were generated based on the crystal structures of various extracellular LRR proteins and subsequently up-dated using the crystal structure of mouse TLR4 (18). Briefly, individual domains of the TLR4 ectodomain that had a high degree of similarity with different known structures were modeled separately and subsequently combined in silico using overlapping regions. The reconstructed full-length ectodomain was further energy minimized in MODELLER. For all TLR4 and MD-2 models, electrostatic potentials were calculated using the AMBER force field via the PDB2PQR server at agave.wustl.edu/pdb2pqr/server.html and the electrostatic calculation program APBS that provides the numerical solution of the Poisson-Boltzmann equation. Visualization was achieved in PyMol (www.pymol.org). The presence and features of pockets was analyzed using the online CastP server (31).

Low resolution protein-protein docking was conducted on the crystal structure of the mouse MD-2/TLR4 complex (Protein Data Bank code 2Z64) using GRAMM (Global RAnge Molecular Matching) methodology (32). GRAMM methodology is an empirical approach to smoothing the intermolecular energy function by changing the range of the atom-atom potentials. Low resolution docking is useful for determining the possible relative positions of the two proteins in the complex. High-resolution protein-protein docking was performed by the program pyDock (33). pyDock is a method for rigid-body protein-protein docking. It explores with either the FTDOCK or the ZDOCK method to generate conformations of complexes and uses a scoring function that applies electrostatics and desolvation energies to select the hundred best solutions. The PROBE program was used to evaluate protein-protein and protein-ligand contacts (34). The approach is based on a probe of radius 0.25 Å placed at points along the van der Waals surface of a selected set of atoms to determine whether this probe also contacts atoms within a second "target" set. Atomic coordinates from crystal structures, homology, and docking models were modified in the companion program REDUCE to add hydrogens that are necessary for a meaningful analysis of molecular contact surfaces.

Statistical analysis

Comparison between control and other treatments within each species group were made using Welch's *t* test for comparing two samples with unequal variances and a Holm-Bonferroni step-down adjustment for multiple comparisons. Only data with significant differences are discussed in the text, where significance is taken at a level of at least $p < 0.05$. Comparisons across species groups were made using a linear regression model. A table of *p* values (Table S1) is presented as supplemental data.[5]

Results

Determinants in both MD-2 and TLR4 contribute to ligand recognition

Preliminary studies suggested that, as in the mouse, lipid IVa has agonist activity in horse (equine) macrophages (data not shown). We constructed dose-response curves for human, mouse, and horse MD-2/TLR4 to lipid A and lipid IVa. Lipid A activated both human and horse MD-2/TLR4 whereas lipid IVa was an agonist to mouse, a partial agonist to horse, and an antagonist to human MD-2/TLR4 (Fig. 1*A*). In the rest of this study we used a concentration of lipid A (10 ng/ml; 4.5 nM) that induced just submaximal activation of pNF-κB-luc and lipid IVa at 1 μg/ml (711 nM; a concentration that just maximally activated murine and horse MD-2/TLR4 but also antagonized lipid A activation of human MD-2/TLR4). Surface expression of TLR4 was equal for the horse and human constructs, but there were slight differences in expression for the intracellular levels of this protein. The differences in intracellular expression of TLR4 were not reflected in cell surface expression, but in all subsequent experiments lipid A stimulation was performed to ensure that the MD-2/TLR4 constructs were able to signal and to control for any differences in protein expression. By focusing our study on the effectiveness of lipid IVa as an agonist or antagonist against lipid A, we were able to characterize a change in pharmacological phenotype in response to MD-2/TLR4 stimulation rather than simply detect a loss of signaling.

To determine whether MD-2 confers the observed species-specific differences in signaling, we conducted a series of MD-2/TLR4

[5] The online version of this article contains supplemental material.

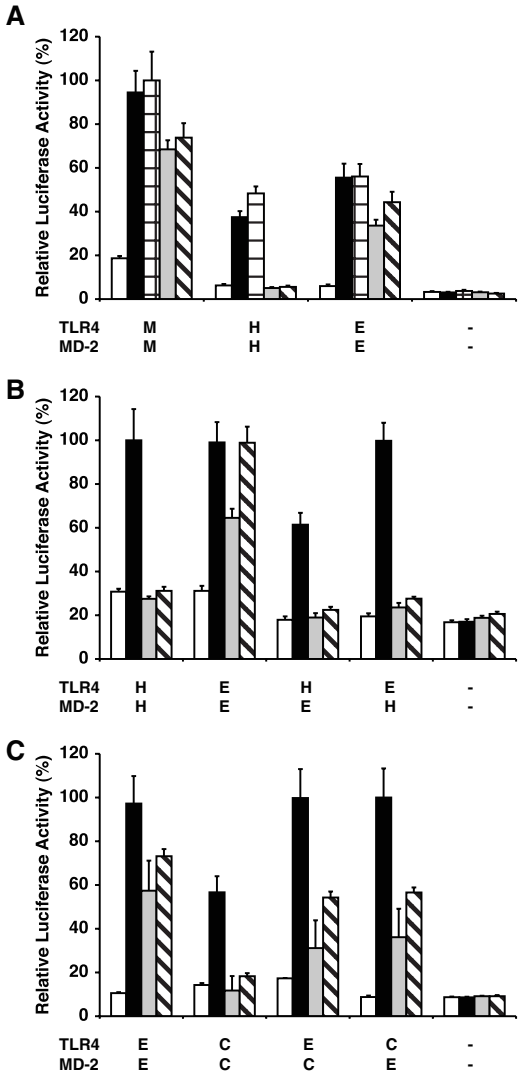

FIGURE 1. Signaling characteristics of MD-2/TLR4 from human, horse, and cat. HEK293 cells were transiently cotransfected with TLR4, MD-2, and CD14 from horse (E), human (H), mouse (M), or cat (C), an NF-κB luciferase reporter plasmid, and a control *Renilla*-expressing plasmid. Cells were stimulated with lipid A, lipid IVa, or both in combination. Unstimulated control (open bar), lipid A at 10 ng · ml^{-1} (black bar), lipid A at 100 ng · ml^{-1} (horizontal hatched bar), lipid IVa at 1 μg · ml^{-1} (gray bar), and lipid A at 10 ng · ml^{-1} plus lipid IVa at 1 μg · ml^{-1} (cross hatched bar) are shown. Data are expressed a percentage of the control response ± SEM from a representative experiment (n = 3–5). *A*, Lipid IVa is a partial agonist at horse MD-2/TLR4 (E). *B*, Neither horse MD-2 (E) nor horse TLR4 (E) alone confers responsiveness to lipid IVa. *C*, Lipid IVa is an antagonist at cat TLR4/MD-2 (C) but a partial agonist at horse TLR4 (E)/cat MD-2(C) and at cat TLR4 (C)/horse MD-2 (E).

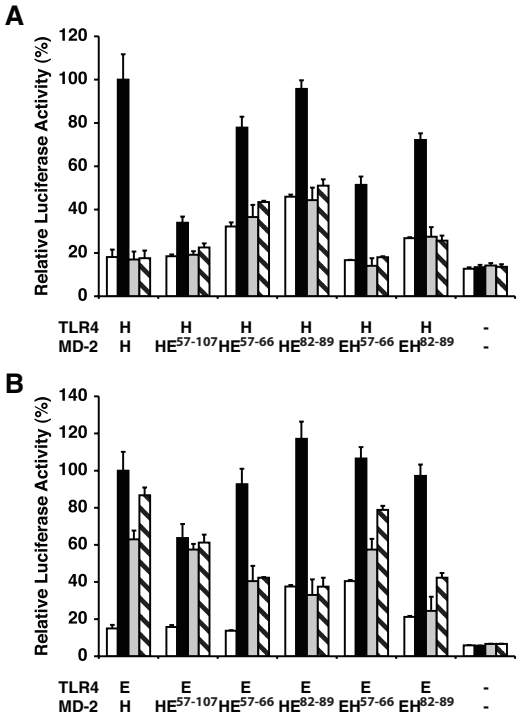

FIGURE 2. A discrete sequence in MD-2 is sufficient to confer responsiveness to lipid IVa. HEK293 cells were transfected with a horse-human MD-2 chimera together with human (H) (*A*) or horse (E) (*B*) TLR4, CD14, an NF-κB luciferase reporter plasmid, and a control *Renilla* expressing plasmid. Transfected cells were stimulated with lipid A, lipid IVa, or both together. Unstimulated control (open bar), lipid A at 10 ng · $ml^{-}1$ (black bar), lipid IVa at 1 μg · ml^{-1} (gray bar), lipid A at 10 ng · ml^{-1} plus lipid IVa at 1 μg · ml^{-1} (cross hatched bar) are shown. Data are expressed as a percentage of the control response ± SEM from a representative experiment (n = 3–5).

swapping experiments and assayed for agonism or antagonism by lipid A and lipid IVa. We asked whether horse MD-2 could confer signaling in response to lipid IVa on human TLR4 and vice versa. Both of these combinations result in TLR4/MD-2 complexes that signal strongly in response to lipid A but are antagonists for lipid IVa (Fig. 1*B*), indicating that MD-2 alone cannot confer the ability to be activated by lipid IVa. Cats, like mice, are relatively less sensitive to LPS than humans or horses in vivo. Cat TLR4/MD-2 has similar properties as those of the human receptor complex, with lipid IVa acting as an antagonist as does cat TLR4 when combined with human MD-2. Cat MD-2/horse TLR4 and horse MD-2/cat TLR4 combinations, in contrast, are activated by lipid IVa (Fig. 1*C*). This result provides further evidence that signaling competency involves determinants in both MD-2 and TLR4.

Residues 57–107 of horse MD-2 are sufficient to confer agonist activity of lipid IVa

Species differences in activation by lipid IVa may depend on a short sequence in MD-2. We constructed MD-2 chimeras in which different regions were switched between human and horse proteins. The chimera in which residues 57–107 of horse MD-2 were engineered into the human framework (HE^{57-107}) was unable to signal in response to lipid IVa when combined with human TLR4 but reconstituted signaling when coexpressed with horse TLR4 (Fig. 2). Thus, residues 57–107 of horse MD-2 are critical for recognition of lipid IVa as an agonist (compare with Fig. 1*B*).

When residues 57–66 of human MD-2 were replaced by the horse sequence (HE^{57-66}), this construct was also able to reconstitute lipid IVa signaling with horse TLR4 but to a lower level than that seen with HE^{57-107} (Fig. 2*B*). A third chimera containing residues 82–89 of the horse MD-2 sequence (HE^{82-89}) retained the lipid IVa antagonist activity both with human and horse TLR4 (Fig. 2). When the reciprocal chimera in which a horse MD-2 with human residues 57–66 (EH^{57-66}) was constructed, it reduced the ability of horse TLR4 to signal in response to lipid IVa (note the elevated activity of the unstimulated cells) (Fig. 2*B*). Introducing human residues 82–89 into the horse MD-2 (EH^{82-89}) did not alter the signaling profiles (Fig. 2). Taken together, these results suggest

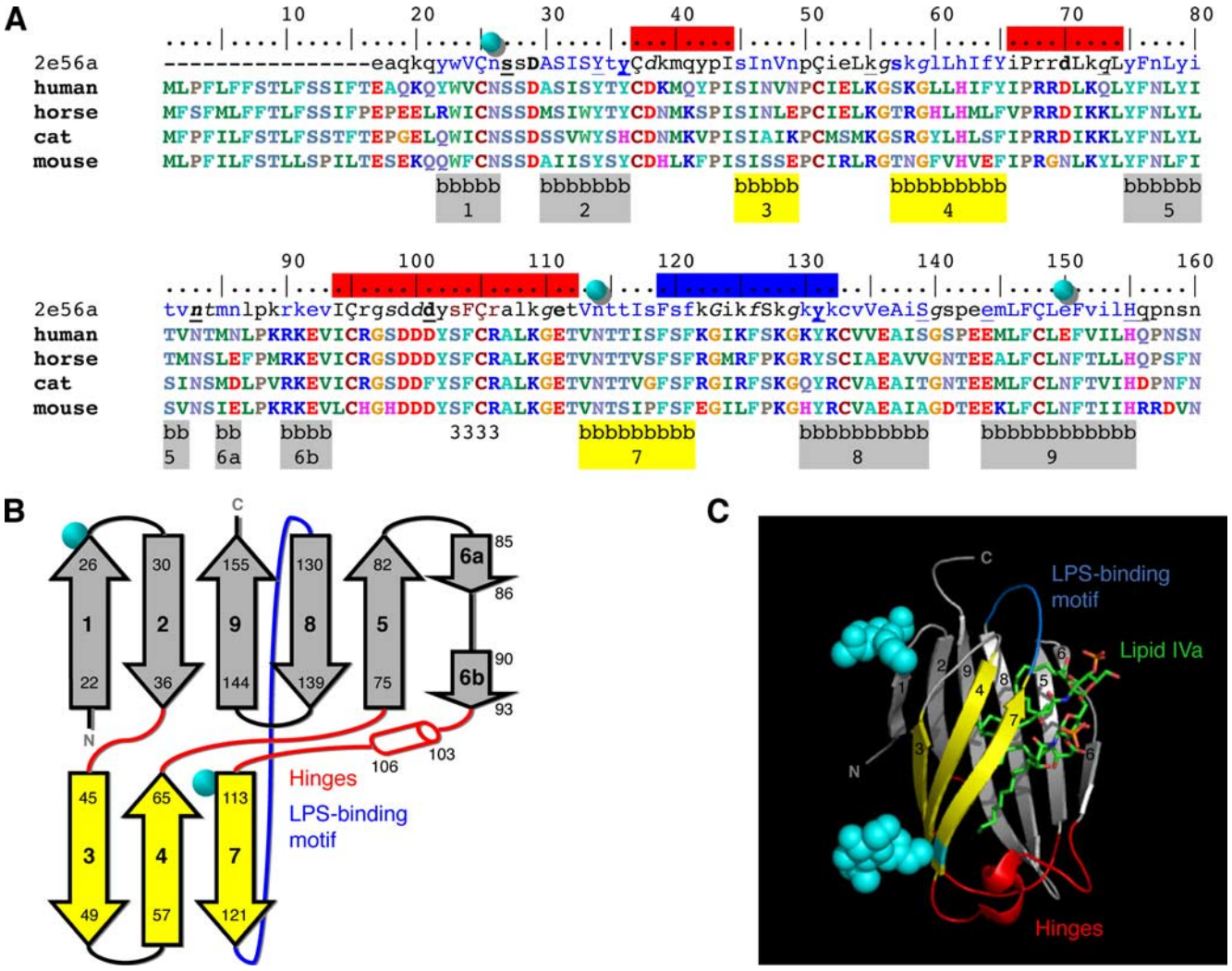

FIGURE 3. MD-2 sequence and structure. *A*, Sequence-structure alignment of MD-2 from different species in which 2e56a stands for the human MD-2 crystal structure with PDB code 2e56, chain a, shown in the JOY format. The alignment was built in BioEdit (www.mbio.ncsu.edu/BioEdit/bioedit.html). *B*, Topological diagram of the MD-2 structure adapted from TOPS output (www.tops.leeds.ac.uk/). Arrows represent β-strands, the cylinder represents the 3_{10} helix, the full lines represent loops, and the purple circles represent glycosylation sites. MD-2 is composed of two antiparallel β-sheets; the first one is formed by β-strands 1/2/9/8/5/6 in gray and the second one encompasses β-strands 3/4/7. These β-sheets form a ligand-binding clam with four hinges (red and blue lines). The blue hinge between β-strands 7/8 carries the LPS binding motif. *C*, A ribbon diagram of MD-2 crystal structure, color-coded as in *B*. Glycans at positions N26 on β-strand 1 and N114 on β-strand 7 are represented in purple spheres. Note that horse, cat, and mouse have a supplementary glycosylation site at N150.

that residues 57–106 of MD-2 determine species specificity in LPS signaling.

Modeling of MD-2 reveals structural differences in surface electrostatic potential that correlate with species specificity in lipid IVa pharmacology

To determine whether sequence differences in MD-2 explain the variations described above, we performed structure based sequence alignments and generated molecular models of the horse, mouse, and cat MD-2 molecules to investigate their molecular structure (Figs. 3 and 4). In agreement with the high sequence identity among MD-2 proteins from different mammalian species (64–66% identity with human MD-2; Fig. 3), no major structural differences were found in the overall folds of these proteins.

Our mutagenetic analysis of MD-2 reveals that sequence differences found in the central region of MD-2 are important for lipid IVa signaling. Residues 57–107 of MD-2 encompass β-strands 4, 5, 6a, and 6b, the 3_{10} helix and the surrounding loops that make contact with lipid IVa (Fig. 4). Replacement of residues 57–66 and 82–89 of horse MD-2 with the human sequence generated a constitutively active form of MD-2 (Fig. 2). The elements of secondary structure that have been switched between species are located on either side of the MD-2 clamshell; residues 82–89 participate in β-strand 6a, which is found on the first sheet at the rim of the ligand-binding pocket, and residues 57–66 constitute β-strand 4, which is in the middle of the second sheet. They present six and seven amino acid changes respectively, in contrast to the 15 changes in total in the central region. These residues are either exposed to solvent or are lining the central cavity, and four of them are in direct contact with lipid IVa in the crystal structure (from human to horse: I63M and Y65F on β-strand 4 and V82M and L87F on β-strand 6a). These changes are mostly conserved in terms of hydropathy (for example, human S57 is replaced by horse T57), whereas polarity changes can be found on solvent-exposed residues (from human to horse: L60H on β-strand 4 and N86E and K89M on β-strand 6).

Comparison of the surface charge distribution of MD-2 from the different species show significant differences in the electrostatic

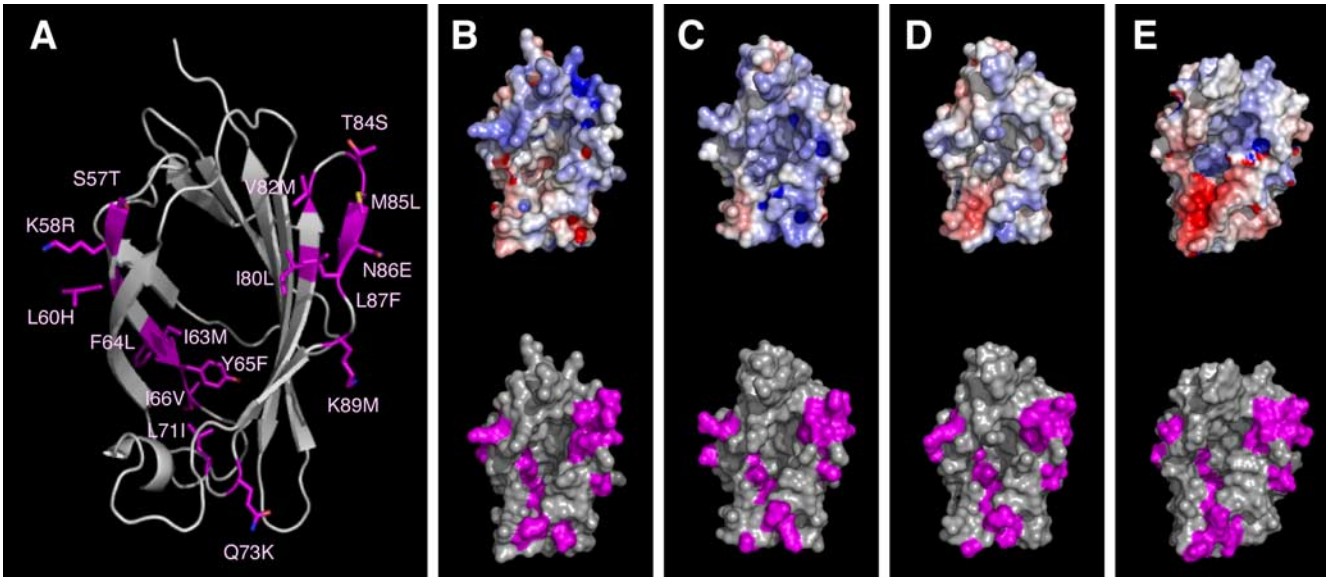

FIGURE 4. Distinct electrostatic surface potentials of MD-2 from different species. *A*, Human MD-2 is shown in ribbon representation with residues 57–66 and 82–89, which vary between human and horse, highlighted in magenta. Residues 57–66 are located on β-strand 4. Residues 82–89 are located on β-strand 6a and the surrounding loops that line up the opening of the ligand-binding cavity. *B–E*, Electrostatic surface potentials are represented for human (*B*), cat (*C*), horse (*D*), and mouse (*E*) proteins. Human MD-2 protein was taken from the crystal structure with PDB code 2Z65. Models for cat and horse proteins were built using the human MD-2 crystal structure (PDB code 2E54). Mouse MD-2 was taken from the crystal structure with PDB code 2Z64.

potential around the ligand-binding cavity (Fig. 4). These differences in surface charges could correlate with the pharmacology of lipid IVa, which is an antagonist in the presence of the electronegative human MD-2, a partial agonist with the less electronegatively charged cat and horse proteins, and a full agonist with the more electropositive mouse MD-2 (Figs. 4). We cannot, however, rule out that the residues we have modified are involved in altered protein dynamics rather than modified ligand and/or TLR4 binding properties.

LRRs 14–18 of the TLR4 ectodomain are required for species-specific responses to lipid IVa

The TLR4 ectodomain is made up of 21 LRRs forming a horseshoe-shaped block surrounded by cysteine-rich capping structures called LRRNT at the N terminus and LRRCT at the C terminus (20) (Figs. 5 and 6). These structures protect not only the first and last repeats from solvent exposure but also have important functional roles in signaling. Homodimerization of TLR4 leads to the

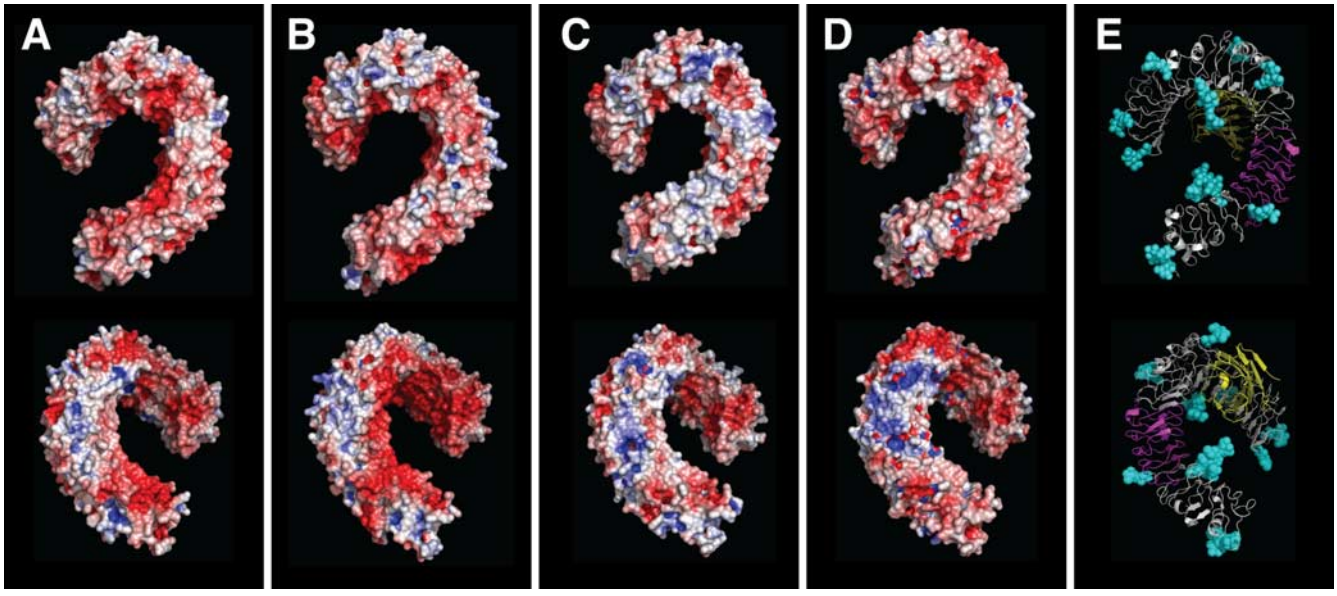

FIGURE 5. Species-specific charge distribution on the surface of the TLR4 ectodomain. The right (*top panels*) and left flanks (*bottom panels*) of the TLR4 ectodomains are represented for human (*A*), cat (*B*), horse (*C*), and mouse (*D* and *E*) proteins. As for MD-2, the electrostatic surface potentials of the TLR4 ectodomains (*A* to *D*, respectively) vary greatly among species. TLR4 LRRs 14–18 are highlighted in magenta in the ribbon diagram (*E*); MD-2 is shown in yellow and TLR4 *N*-linked glycans are depicted in cyan. Human, cat, and horse TLR4 ectodomains were modeled on the mouse TLR4 crystal structure (PDB code 2Z64).

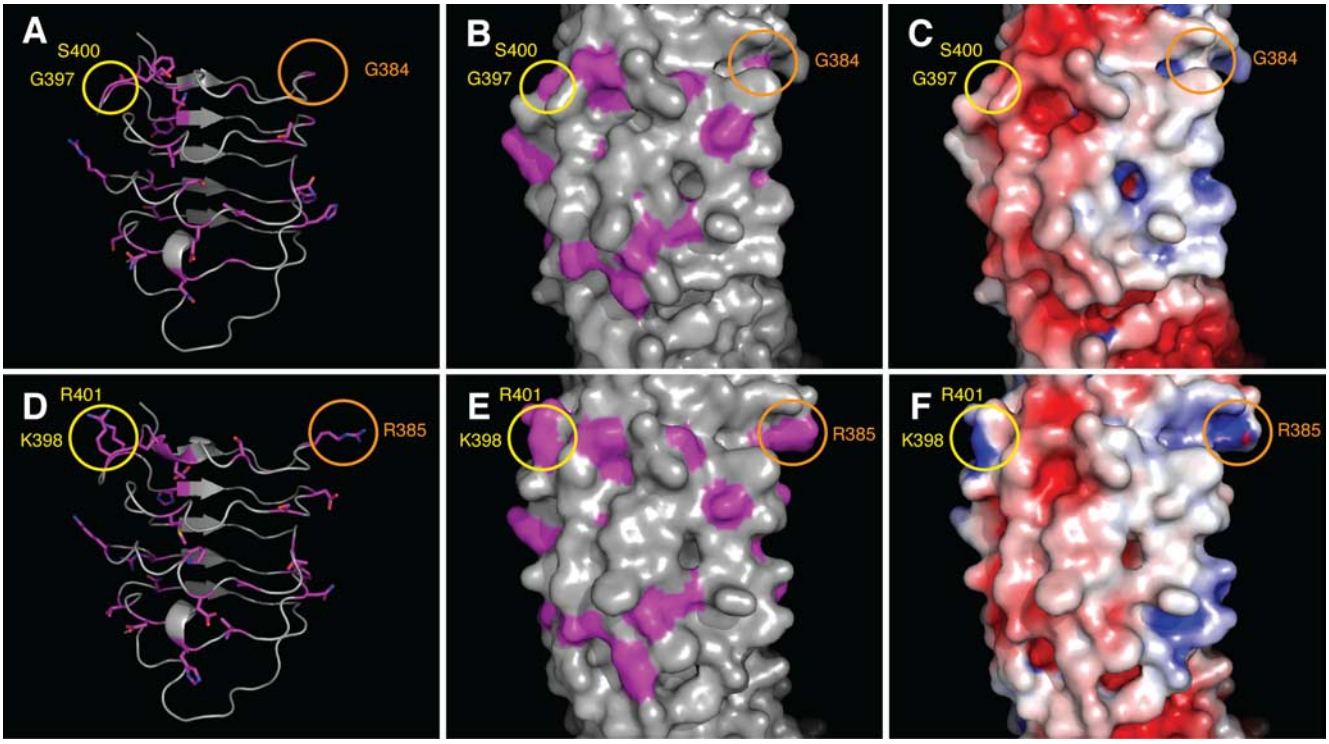

FIGURE 6. TLR4 LRRs 14–18 present species differences in shape and electrostatic surface potentials. The convex sides of human (*A*, *B*, and *C*) and horse (*D*, *E*, and *F*) TLR4 LRRs 14–18 are represented as ribbon diagrams (*A* and *D*, respectively) and molecular surface representations (*B* and *E*) with species-specific residues shown in magenta and electrostatic surface potential (*E* and *F*, respectively). Encircled residues have been swapped between human and horse proteins. In yellow circles, horse TLR4 K398G and R401S "humanized mutants" on the left flank of the LRR motif did not affect lipid IVa activity. In orange circles, the horse TLR4 R385G "humanized" mutant localized on the right flank lost the ability to signal with lipid IVa.

activation of an intracellular signaling cascade (35). However, it is unclear whether TLR4 dimerization is triggered directly by MD-2 bound to a ligand or whether the receptor undergoes allosteric changes upon MD-2-ligand binding. The latter scenario would involve receptor-receptor contacts in which ligand-bound MD-2 may or may not participate. If ligand-bound MD-2 participates in receptor-receptor contacts, it would explain why TLR4 may play a role in ligand recognition.

To determine the role of the TLR4 ectodomain in lipid IVa signaling, we made chimeras between horse and human proteins. Hybrids in which the human LRR 14-TIR (Toll-IL-1R) domain (L372–D675) was replaced with the corresponding residues from horse ($HE^{L373–D677}$) and the reciprocal construct in which the horse LRR 14-TIR (L373–D677) domain was replaced with the corresponding residues from human ($EH^{L372–D675}$) were generated and their signaling activity characterized. Lipid IVa acts as an agonist for $HE^{L373–D677}$and an antagonist for $EH^{L372–D675}$ (Fig. 7*A*). This result confirms that TLR4, specifically the C terminus from LRR 14, is essential for lipid IVa signaling. To localize the regions of TLR4 involved, we assayed chimeras with only LRRs 14–18 swapped between human (L372–V475) and horse (L373–V476) receptors ($HE^{L373–V476}$ and $EH^{L372–V475}$, respectively). These experiments showed that LRRs 14–18 are sufficient to confer responsiveness to lipid IVa (Fig. 7*B*).

Sequence comparison of horse and human LRRs 14–18 highlighted 12 nonconservative amino acid changes, of which eight involved substitution of neutral residues in the human sequence with charged residues in the horse (see Fig. 6 at the following positions for human/horse residues: G384/R385, Q393/E394, G397/K398, S400/R401, Y403/H404, G410/D411, I450/R451, and N468/D469). We therefore introduced point mutations into the horse sequence corresponding to these residues and tested the mutated TLR4 for the ability to confer responsiveness to lipid IVa. Remarkably, one of these substitution, R385G in LRR 14, despite being fully active in response to lipid A, results in a receptor complex with markedly reduced signaling in response to lipid IVa ($p = 7.7 \times 10^{-7}$). Moreover, lipid IVa antagonizes the effects of lipid A at horse TLR4 R385G (Fig. 7*C*). A second mutation at this site (R385A) also reduced lipid IVa activity while retaining the antagonist effect of lipid IVa against lipid A (data not shown). This residue lies on the right-hand lateral surface of the LRR solenoid. Other mutants involving basic residues located on the left-hand lateral surface had unaltered signaling properties (data not shown). These results implicate the right-hand lateral surface of horse TLR4 as a region essential for lipid IVa but not lipid A signaling.

MD-2/TLR4 and TLR4/TLR4 interactions contribute to the formation of the TLR4/MD-2 signaling complex

The structure of mouse TLR4 in complex with mouse MD-2 without any added ligand and the human TLR4 N-terminal domain with MD-2 bound to the tetra-acylated antagonist eritoran have been solved (18). The MD-2/TLR4 interface of these inactive complexes lies outside of the species-specific regions identified here (Table I). To explore the significance of LRRs 14–18 of the TLR4 solenoid for the formation of an active complex, we used the molecular docking programs GRAMM and pyDock (Tables I–VI). We generated different docking models of the heterotetrameric complex using the mouse MD-2/TLR4 crystal structure as a template. We selected signaling complexes that present a 2-fold symmetry axis perpendicular to the cell surface and in which the TLR4 juxtamembrane domains are in close proximity.

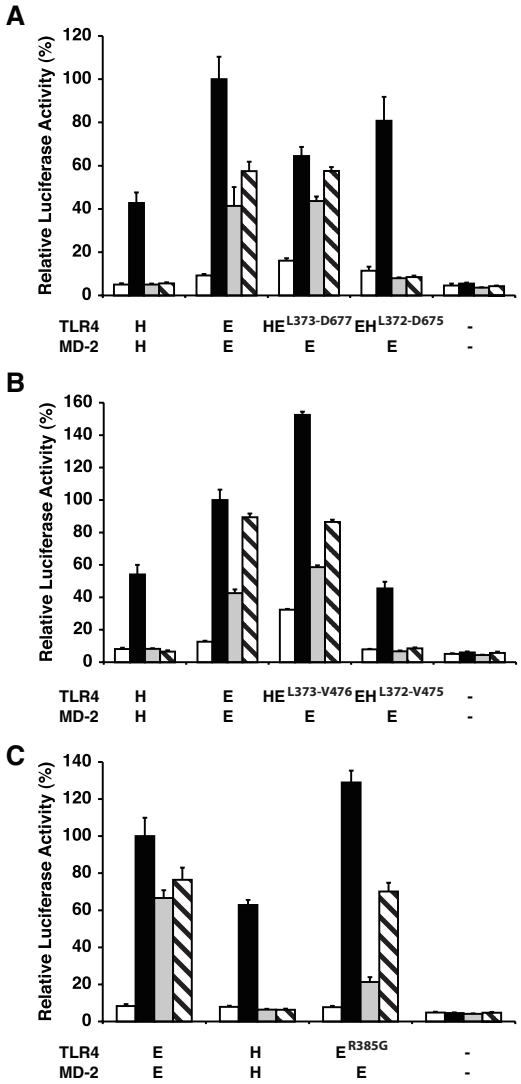

FIGURE 7. Sequences in LRRs 14–18 of TLR4 are required for signaling in response to lipid IVa. HEK293 cells were transfected with horse-human TLR4 chimeras together with human (H) or horse (E) MD-2, CD14, an NF-κB luciferase reporter plasmid, and a control *Renilla*-expressing plasmid. The transfected cells were stimulated with lipid A, lipid IVa, or both together. Unstimulated control (open bar), lipid A at 10 ng $\cdot$ ml^{-1} (black bar), lipid IVa at 1 μg $\cdot$ ml^{-1} (gray bar) and lipid A at 10 ng $\cdot$ ml^{-1} plus lipid IVa at 1 μg $\cdot$ ml^{-1} (cross hatched bar) are shown. Data are expressed as a percentage of the control response $\pm$ SEM from a representative experiment (n = 3–5). *A*, Replacement of L372 (in LRR 14) to D675 of human TLR4 with L373–D677 of horse TLR4 (HE$^{L373-D677}$) permits lipid IVa signaling. *B*, Replacement of L373 (in LRR 14) to V476 (in LRR 18) of horse TLR4 with L372–V475 of human TLR4 (EH$^{L372-V475}$) makes lipid IVa an antagonist. *C*, Mutation of R385G in horse (E^{R385G}) TLR4 markedly reduces lipid IVa signaling at horse TLR4/MD-2.

These two parameters are thought to be required for assembly of the MD-2/TLR4 signaling complex. Some of the models filled both the criteria of symmetry and proximity of the C-termini of the two TLR4 solenoids, but also involved TLR4/TLR4 interactions and MD-2 crosslinking of two receptor molecules. One of these docking models (Fig. 8) suggests a TLR4 interface located on the right-hand lateral surface and centered at LRR 14 as a site of receptor homodimerization (see Fig. 8*C*, where points of contact are illustrated in orange, and *E,* where LRRs 14–18 are in magenta). The critical residue R385G in horse TLR4, which determines the activity of lipid IVa (shown in blue in Fig. 8*E*), is located within this patch, suggesting that the presence of a basic residue in the horse sequence can promote the formation of the receptor-receptor contacts required for signal transduction. Another interesting feature of this model resides in the interchain contacts between MD-2 and TLR4, and this may also contribute to the formation of the

Table I. *The MD-2 binding site on TLR4 is highly conserved among species*[a]

LRR	mTLR4	hTLR4	eTLR4	fTLR4
LRRNT	M40	M41	M41	M41
LRR 1	D59	D60	D60	D60
LRR 1	F62	F63	F63	F63
LRR 2	D83	D84	D84	D84
LRR 2	S85	S86	S86	S86
LRR 2	R86	R87	R87	R87
LRR 3	T109	T110	T110	T110
LRR 4	V131	V132	V132	V132
LRR 4	V133	V134	V134	V134
LRR 4	E134	E135	E135	E135
LRR 5	H158	H159	H159	H159
LRR 7	S210	S211	S211	S211
LRR 7	L211	L212	L212	L212
LRR 9	F262	F263	F263	F263
LRR 9	K263	**R264**	K264	K264
LRR 9	**D264**	N265	N265	N265
LRR 9	**E265**	E266	E266	E266
LRR 10	R288	R289	R289	R289
LRR 10	**T290**	A291	A291	A291
LRR 12	**I336**	V338	V338	V338
LRR 12	**R337**	N340	N340	N339
LRR 13	**M358**	S360	S361	S360

[a] Residues from mouse TLR4 in contact with mouse MD-2 in the crystal structure (Protein Data Bank no. 2z64) are listed. Equivalent residues in human, horse, and cat TLR4s according to sequence alignment are presented; mTLR4, mouse TLR4; hTLR4, human TLR4; eTLR4, horse (equine) TLR4; and fTLR4, cat (felix) TLR4. The far left column indicates the structural localization of each residue spanning from the N-terminal region (LRRNT) to LRR 13. Residues from LRR 9 to LLR 14 in boldface are less conserved among species.

Table II. *The TLR4 binding site on MD-2 is highly conserved among species*[a]

Structure	mMD-2	hMD-2	eMD-2	fMD-2
L4-5	I66	I	V	I
L4-5	R68	R	R	R
L6b-3_{10}	**H96**	R	R	R
L6b-3_{10}	**H98**	S	S	S
L6b-3_{10}	D99	D	D	D
L6b-3_{10}	D101	D	D	F
L6b-3_{10}	Y102	Y	Y	Y
3_{10}	S103	S	S	S
3_{10}	F104	F	F	F
3_{10}	R106	R	R	R
$L3_{10}$-7	L108	L	L	L
$L3_{10}$-7	K109	K	K	K
$L3_{10}$-7	G110	G	G	G
$L3_{10}$-7	E111	E	E	E
$L3_{10}$-7	T112	T	T	T
7	I117	I	V	V
7	**P118**	S	S	**G**

[a] Residues from mouse MD-2 in contact with mouse TLR4 in the crystal structure (Protein Data Bank no. 2z64) are listed. Equivalent residues in human, horse, and cat MD-2s are presented according to sequence alignment: mMD-2, mouse MD-2; hMD-2, human MD-2; eMD-2, horse (equine) MD-2; and fMD-2, cat (felix) MD-2. The far left column indicates the structural localization of each residue; L4-5, loop (L) between the fourth and fifth β-strand; 3_{10}, 3_{10} helix; 6b, β-strand 6b. Residues involved in both TLR4 and ligand binding are underlined. Residues that are not conserved are shown in boldface.

Table III. *The ligand-binding site of MD-2 is mostly conserved among species*[a]

Structure	Position	HMD-2	mMD-2	eMD-2	fMD-2
3	46	I	I	I	I
3	**48**	**V**	**S**	**L**	**I**
L3-4	52	I	I	I	**M**
L3-4	54	L	L	L	**M**
4	61	L	**V**	L	L
4	**63**	**I**	**V**	**M**	**L**
4	**65**	**Y**	F	F	F
L4-5	71	L	L	**I**	**I**
5	76	F	F	F	F
5	78	L	L	L	L
5	80	I	I	L	**L**
L6a-6b	87	L	L	**F**	L
L6b-3_{10}	102	Y	Y	Y	Y
3_{10}	104	F	F	F	F
7	113	V	V	V	V
7	117	I	I	**V**	**V**
7	119	F	F	F	F
7	120	S	S	S	S
7	121	F	F	F	F
L7-8	**122**	**K**	**E**	R	R
L7-8	123	G	G	G	G
L7-8	124	I	I	M	I
8	133	C	C	C	C
8	**135**	**V**	A	A	A
9	146	L	L	L	L
9	147	F	F	F	F
9	151	F	F	F	F

[a] The ligand-binding site of MD-2 is mostly conserved among species. Residues from human MD-2 in contact with eritoran in the crystal structure are listed (Protein Data Bank no. 2z65). Equivalent residues in mouse, horse, and cat MD-2s are presented according to sequence alignment: mMD-2, mouse MD-2; hMD-2, human MD-2; eMD-2, horse (equine) MD-2; and fMD-2, cat (felix) MD-2. The far left column indicates the structural localization of each residue; L4-5, loop (L) between the fourth and fifth β-strand; 3_{10}, 3_{10} helix; 6b, β-strand 6b. Residues that are not conserved are shown in boldface.

signaling complex (see Fig. 8, *B* and *C*, with MD-2/TLR4 interchain contacts illustrated in green). The interactions occur on the concave surface of the TLR4 solenoid between LRRs 16–18. Interestingly, the F126 residue of MD-2 that is critical for

Table IV. *The docking study of heterotetrameric TLR4/MD-2_2 complex suggests potential TLR4-TLR4 contacts*[a]

Structure	mTLR4	hTLR4	ETLR4	fTLR4
LRR12	**K341**	**G343**	E344	E344
LRR12	Q342	Q344	**G345**	Q344
LRR13	G361	G363	**D364**	**V363**
LRR13	**S362**	**G364**	**M365**	**R364**
LRR13	**S364**	A366	**S367**	A366
LRR13	**K366**	**S368**	**N369**	**T368**
LRR13	**K367**	E369	E370	**Q369**
LRR14	**A382**	**G384**	**R385**[b]	**D384**
LRR14	S384	S386	S387	S386
LRR14	S386	K388	K389	K388
LRR15	**I411**	T413	**S414**	T413
LRR16	**E437**	**E439**	D440	D439
LRR16	F438	F440	F441	F440

[a] The docking study of the heterotetrameric TLR4/MD-2_2 complex suggests potential TLR4-TLR4 contacts. Docking analysis was performed on the mouse TLR4-mouse MD-2 complex using the crystal structure with Protein Data Bank no. 2Z64 coordinates as both "receptor" and "ligand" using the GRAMM-X web server (vakser.bioinformatics.ku.edu/resources/gramm/grammx/). Equivalent residues in human, horse, and cat TLR4s according to sequence alignment are presented; mTLR4, mouse TLR4; hTLR4, human TLR4; eTLR4, horse (equine) TLR4; and fTLR4, cat (felix) TLR4. The far left column indicates the structural localization of each residue spanning from LRR 12 to LRR 16. Note that the TLR4-TLR4 interface is highly divergent among species. Residues that are not conserved are indicated in boldface.

Table V. *The docking study of heterotetrameric TLR4/MD-2_2 complex suggests the presence of a secondary MD-2 binding site on TLR4*[a]

Structure	Mouse	Human	Horse	Cat
LRR15	N415	N417	N418	N417
LRR15	**M417**	L419	**M420**	L418
LRR16	G418	G420	G421	G420
LRR16	**T436**	S438	S439	S438
LRR16	**E437**	**E439**	D440	D439
LRR16	F438	F440	F441	F440
LRR16	L442	L444	L445	L444
LRR17	S443	S445	S446	**P445**
LRR17	E445	**R447**	K448	K447
LRR17	**D460**	A462	**V463**	A462
LRR17	F461	F463	F464	F463
LRR17	**D462**	**N464**	H465	H464
LRR17	**L466**	N468	**D469**	N468

[a] The docking study of the heterotetrameric TLR4/MD-2_2 complex suggests the presence of a secondary MD-2 binding site on TLR4. Docking analysis was performed on the mouse TLR4-mouse MD-2 complex using the crystal structure with Protein Data Bank no. 2Z64 coordinates as both "receptor" and "ligand" using the GRAMM-X web server (vakser.bioinformatics.ku.edu/resources/gramm/grammx/). Equivalent residues in human, horse, and cat TLR4s according to sequence alignment are presented. The far left column indicates the structural localization of each residue spanning from LRR 15 to LRR 17. Residues that are not conserved are indicated in boldface.

LPS-induced TLR4 (36) clustering lies within the MD-2/TLR4 interface predicted by our docking analysis.

The constitutive activity of MD-2 HE^{82-89} can be explained by the docking analysis. Horse residues in the 82–89 region are slightly more hydrophobic and bulkier than those in human MD-2, in particular at position 87, which is a Phe residue in horse and a Leu in human (Table VI). Our data show that this mutant with high basal activity can still be further stimulated with lipid A. Taken together, this suggests that a more extensive range of contacts than those proposed (18) occur in the signaling complex. The partial activity seen with mutant proteins or lipid IVa stimulation is due to productive protein-protein interactions in some, but not all, possible areas. In contrast, full stimulation would then only be observed when all stabilizing contacts occur between TLR4 and MD-2 in the presence of a full agonist such as lipid A. The introduction of bulkier hydrophobic residues into MD-2 increases the size of this

Table VI. *The docking study of heterotetrameric TLR4/MD-2_2 complex suggests the presence of a secondary TLR4 binding site on MD-2*

Structure	Position	mMD-2	hMD-2	eMD-2	fMD-2
<u>B5</u>	<u>82</u>	V	V	**M**	**I**
<u>B6a</u>	<u>85</u>	**I**	M	**L**	M
<u>L6a-6b</u>	<u>87</u>	L	L	**F**	L
<u>L6a-6b</u>	<u>88</u>	P	P	P	P
<u>B6b</u>	<u>90</u>	R	R	R	R
L7–8	123	G	G	G	G
L7–8	124	I	I	**M**	I
L7–8	125	**L**	**K**	R	R
L7–8	126	F	F	F	F
L7–8	128	K	K	K	K

[a] The docking study of the heterotetrameric TLR4/MD-2_2 complex suggests the presence of a secondary TLR4 binding site on MD-2. Docking analysis was performed on the mouse TLR4-mouse MD-2 complex using the crystal structure with Protein Data Bank no. 2Z64 coordinates as both "receptor" and "ligand" using the GRAMM-X web server (vakser.bioinformatics.ku.edu/resources/gramm/grammx/). Equivalent residues in human, horse, and cat MD-2s according to sequence alignment are presented; mMD-2, mouse MD-2; hMD-2, human MD-2; eMD-2, horse (equine) MD-2; and fMD-2, cat (felix) MD-2. The far left column indicates the structural localization of each residue. Residues that have been switched between human and horse in this study belong to the secondary interface (underlined). Note that the rest of the secondary TLR-binding region is located in the LPS binding motif (see Fig. 3). Residues that are not conserved are indicated in boldface.

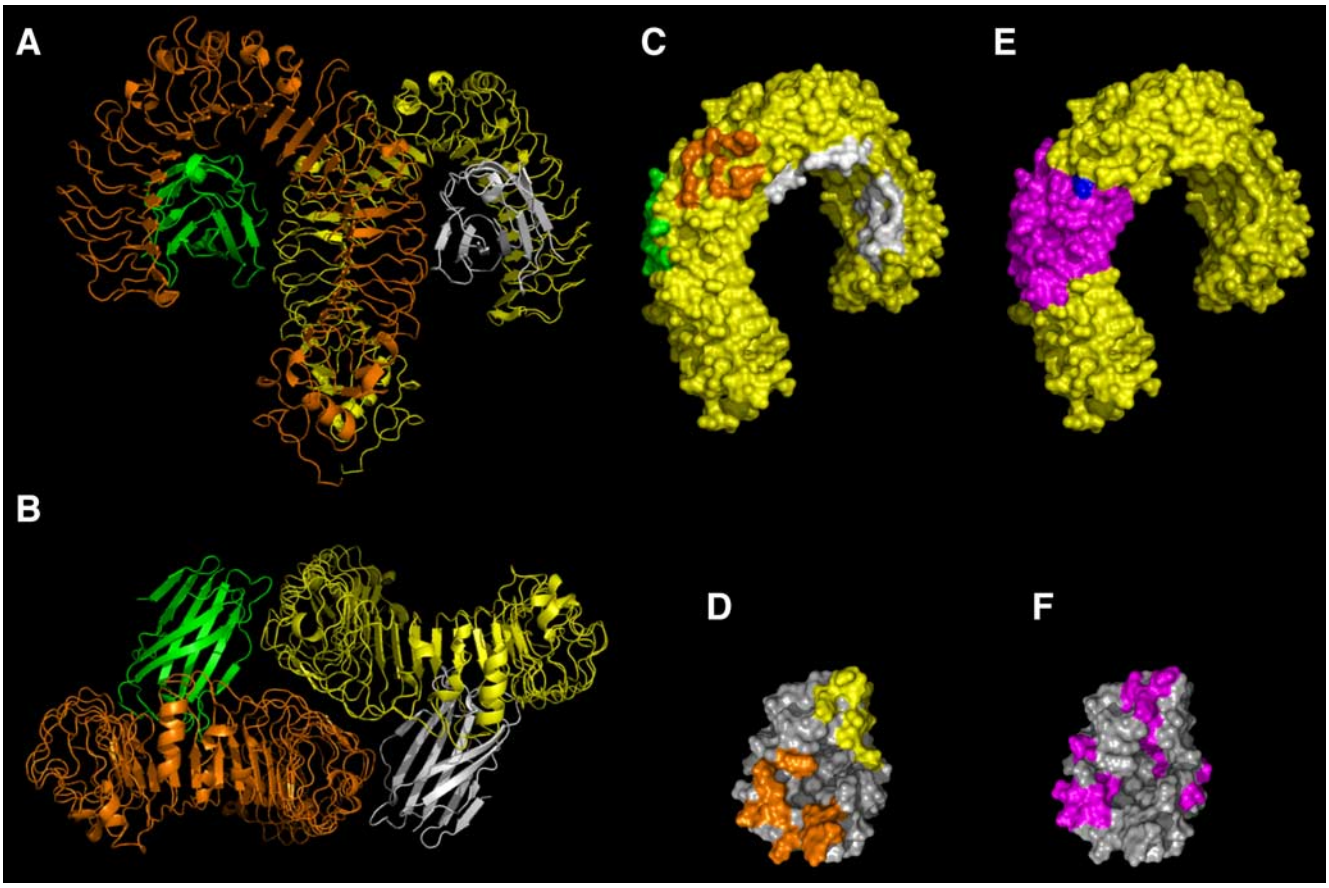

FIGURE 8. Docking model of the MD-2/TLR4 heterotetramer. *A* and *B*, Side view (*A*) and top view (*B*) of the complex in ribbon representation. The MD-2/TLR4 heterodimer as observed in the mouse crystal structure with PDB code 2Z64 is represented in yellow and white and in orange and green, respectively. *C*, The molecular surface of TLR4 is represented in yellow. The MD-2 binding sites on the TLR4 surface are shown in white (as observed in the crystal structure of the mouse TLR4/MD-2 complex) and in green (according to the docking model). The TLR4-TLR4 docking contacts are shown in orange. *D*, The TLR4-binding sites on MD-2 are represented in yellow (as observed in the crystal structure) and orange (docking model), respectively. *E*, TLR4 LRRs 14–18 are represented in magenta. The localization of the residue in LRR 14 that corresponds to horse R385, conferring lipid IVa responsiveness, is shown in blue. Comparing *C* and *D* reveals that the mutated region encompasses the predicted heterotetramerization interface. *F*, Surface representation of MD-2 is in gray with residue 57–66 and 82–89, which differ among species, shown in magenta. Comparing *D* and *E* reveals an overlap of the mutated residues with those of the TLR4 binding sites.

protein, which, in turn, is able to make partial contacts with TLR4 even in absence of ligand.

Discussion

The modeling, docking, and functional studies of MD-2 and TLR4 presented here suggest that subtle differences in these molecules can have major influences on their signaling function. The sequence differences seen between speciation that supports signaling in response to lipid IVa (mouse, horse, and cat) and speciation that cannot (human) are mainly conservative substitutions that are not predicted to have a large influence on the overall structure of the protein. However, we identified significant differences in the local charge distribution on the surfaces of MD-2 and TLR4 from different species that suggest that electrostatic forces govern the pharmacology of lipid IVa and therefore the mechanism of TLR4 signal transduction.

Our mutational analysis of MD-2 provides evidence that the area involved in the signaling activity of lipid IVa is restricted to the central region of MD-2 (residues 57–106), which includes residues involved in ligand and TLR4 binding. Of particular interest are human residues 57–66 and 82–89, which confer a level of constitutive activity on horse MD-2. This observation can be explained if MD-2 is able to adopt two conformers, one of which is active for signaling. In this view, the mouse and horse MD-2 proteins would be able to switch conformation when bound by lipid IVa. The constitutively active hybrid MD-2 would be viewed as metastable, being able to switch conformation spontaneously without any ligand bound. A conformational switch of this type has been characterized structurally in the related ML fold protein GM2-AP (37). Further structural studies are needed with MD-2 to assess the dynamical properties of this particular protein.

Another important conclusion of this study is that the signaling activity induced by lipid IVa also involves TLR4. The importance of the LRRs 14–18 region is as puzzling as the effect of characterized human polymorphisms at position D299G and T399I (19, 20) because they all reside outside of the MD-2 binding site. The effect of such mutations could be indirect by introducing a structural change in the TLR4 ectodomain such as changing the curvature, the overall twist (as opposed to the planarity described for the TLR3 ectodomain; Ref. 38), or the surface charge distribution.

Our model for activation of TLR4 has features in common with those put forward by Kim et al. (18). Their favored model proposed interchain contacts between MD-2 and TLR4, similar to those seen in our docked complex. Both models are similarly supported by mutagenetic data with two highly conserved residues in MD-2 (F126 and H155) that are critical for receptor dimerization in response to LPS, contributing to TLR4 crosslinking (see Fig. 8*B*). Our model, however, also predicts the presence of receptor-receptor contacts. Thus, it may be that the assembly of the active

TLR4 complex is a stepwise process, with initial MD-2/TLR4 contacts induced by the binding of LPS, promoting the subsequent homodimerization of the receptor ectodomains (35). The "m"-shaped arrangement of the ectodomain chains in the predicted complex is strikingly similar to that seen in the structure of the TLR1/2 ectodomain heterodimer (39). In this case, triacylated lipid binds directly to both TLR2 and TLR1. Two acyl chains are inserted into a hydrophobic cavity in the core TLR2 LRRs 9–11, and the remaining acyl chain binds to TLR1 at an equivalent position in the ectodomain. These lipid-protein interactions appear to stabilize a dimerization interface on the lateral surface of the solenoid extending to LRR 14, the same region relative to the C terminus that we have identified in TLR4. Our model also has features in common with a low-resolution structure of the *Drosophila* Toll receptor ectodomain in complex with Spätzle (the protein ligand for Toll). Spätzle binds to the N terminus of the ectodomain to form a heterodimer. Two heterodimers assemble into a tetrameric complex held together by two regions of protein-protein interactions between the receptor ectodomains, one close to the Spätzle binding site and one at the C terminus (40).

In conclusion, the model of the active TLR4/MD-2 complex supported by mutagenetic evidence provides a new insight in the mechanism of TLR4 activation. The additional interactions between TLR4 and MD-2 described in this paper may account for the picomolar sensitivity in sensing the microbial patterns of this pathway. We propose that partial contacts lead to decreased potency in signaling, which accounts for the species-specific activity of lipid IVa. Our results are consistent with those of Muroi and Tanamoto (23), who conducted an analysis of mouse MD-2. This work, taken together with other recent advances, indicates that the Toll and Toll-like receptors have analogous multistep activation mechanisms.

Acknowledgments

We thank T. Cheng, J. Bell, R. Medzhitov, K. Miyake, P. Tobias, J. Moore, S. Hobbs, and C. Raetz for advice and materials.

Disclosures

The authors have no financial conflict of interest.

References

1. Beutler, B., and E. T. Rietschel. 2003. Innate immune sensing and its roots: the story of endotoxin. *Nat. Rev. Immunol.* 3: 169–176.
2. Raetz, C. R., and C. Whitfield. 2002. Lipopolysaccharide endotoxins. *Annu. Rev. Biochem.* 71: 635–700.
3. Nagai, Y., S. Akashi, M. Nagafuku, M. Ogata, Y. Iwakura, S. Akira, T. Kitamura, A. Kosugi, M. Kimoto, and K. Miyake. 2002. Essential role of MD-2 in LPS responsiveness and TLR4 distribution. *Nat. Immunol.* 3: 667–672.
4. Shimazu, R., S. Akashi, H. Ogata, Y. Nagai, K. Fukudome, K. Miyake, and M. Kimoto. 1999. MD-2, a molecule that confers lipopolysaccharide responsiveness on Toll-like receptor 4. *J. Exp. Med.* 189: 1777–1782.
5. Viriyakosol, S., P. S. Tobias, R. L. Kitchens, and T. N. Kirkland. 2001. MD-2 binds to bacterial lipopolysaccharide. *J. Biol. Chem.* 276: 38044–38051.
6. Gioannini, T. L., A. Teghanemt, D. Zhang, N. P. Coussens, W. Dockstader, S. Ramaswamy, and J. P. Weiss. 2004. Isolation of an endotoxin-MD-2 complex that produces Toll-like receptor 4-dependent cell activation at picomolar concentrations. *Proc. Natl. Acad. Sci. USA* 101: 4186–4191.
7. Gangloff, M., and N. J. Gay. 2004. MD-2: the Toll "gatekeeper" in endotoxin signalling. *Trends Biochem. Sci.* 29: 294–300.
8. Ohto, U., K. Fukase, K. Miyake, and Y. Satow. 2007. Crystal structures of human MD-2 and its complex with antiendotoxic lipid IVa. *Science* 316: 1632–1634.
9. Raetz, C. R., T. A. Garrett, C. M. Reynolds, W. A. Shaw, J. D. Moore, D. C. Smith, Jr., A. A. Ribeiro, R. C. Murphy, R. J. Ulevitch, C. Fearns, et al. 2006. Kdo2-lipid A of *Escherichia coli*, a defined endotoxin that activates macrophages via TLR-4. *J. Lipid Res.* 47: 1097–1111.
10. Re, F., and J. L. Strominger. 2002. Monomeric recombinant MD-2 binds Toll-like receptor 4 tightly and confers lipopolysaccharide responsiveness. *J. Biol. Chem.* 277: 23427–23432.
11. Re, F., and J. L. Strominger. 2003. Separate functional domains of human MD-2 mediate Toll-like receptor 4-binding and lipopolysaccharide responsiveness. *J. Immunol.* 171: 5272–5276.
12. Viriyakosol, S., P. S. Tobias, and T. N. Kirkland. 2006. Mutational analysis of membrane and soluble forms of human MD-2. *J. Biol. Chem.* 281: 11955–11964.
13. Visintin, A., E. Latz, B. G. Monks, T. Espevik, and D. T. Golenbock. 2003. Lysines 128 and 132 enable lipopolysaccharide binding to MD-2, leading to Toll-like receptor-4 aggregation and signal transduction. *J. Biol. Chem.* 278: 48313–48320.
14. Mullen, G. E., M. N. Kennedy, A. Visintin, A. Mazzoni, C. A. Leifer, D. R. Davies, and D. M. Segal. 2003. The role of disulfide bonds in the assembly and function of MD-2. *Proc. Natl. Acad. Sci. USA* 100: 3919–3924.
15. Akashi, S., S. Saitoh, Y. Wakabayashi, T. Kikuchi, N. Takamura, Y. Nagai, Y. Kusumoto, K. Fukase, S. Kusumoto, Y. Adachi, et al. 2003. Lipopolysaccharide interaction with cell surface Toll-like receptor 4-MD-2: higher affinity than that with MD-2 or CD14. *J. Exp. Med.* 198: 1035–1042.
16. Andersen-Nissen, E., K. D. Smith, R. Bonneau, R. K. Strong, and A. Aderem. 2007. A conserved surface on Toll-like receptor 5 recognizes bacterial flagellin. *J. Exp. Med.* 204: 393–403.
17. Omueti, K. O., J. M. Beyer, C. M. Johnson, E. A. Lyle, and R. I. Tapping. 2005. Domain exchange between human toll-like receptors 1 and 6 reveals a region required for lipopeptide discrimination. *J. Biol. Chem.* 280: 36616–36625.
18. Kim, H. M., B. S. Park, J. I. Kim, S. E. Kim, J. Lee, S. C. Oh, P. Enkhbayar, N. Matsushima, H. Lee, O. J. Yoo, and J. O. Lee. 2007. Crystal structure of the TLR4-MD-2 complex with bound endotoxin antagonist eritoran. *Cell* 130: 906–917.
19. Arbour, N. C., E. Lorenz, B. C. Schutte, J. Zabner, J. N. Kline, M. Jones, K. Frees, J. L. Watt, and D. A. Schwartz. 2000. TLR4 mutations are associated with endotoxin hyporesponsiveness in humans. *Nat. Genet.* 25: 187–191.
20. Rallabhandi, P., J. Bell, M. S. Boukhvalova, A. Medvedev, E. Lorenz, M. Arditi, V. G. Hemming, J. C. Blanco, D. M. Segal, and S. N. Vogel. 2006. Analysis of TLR4 polymorphic variants: new insights into TLR4/MD-2/CD14 stoichiometry, structure, and signaling. *J. Immunol.* 177: 322–332.
21. Akashi, S., Y. Nagai, H. Ogata, M. Oikawa, K. Fukase, S. Kusumoto, K. Kawasaki, M. Nishijima, S. Hayashi, et al. 2001. Human MD-2 confers on mouse Toll-like receptor 4 species-specific lipopolysaccharide recognition. *Int. Immunol.* 13: 1595–1599.
22. Kawasaki, K., S. Akashi, R. Shimazu, T. Yoshida, K. Miyake, and M. Nishijima. 2001. Involvement of TLR4/MD-2 complex in species-specific lipopolysaccharide-mimetic signal transduction by Taxol. *J Endotoxin Res.* 7: 232–236.
23. Muroi, M., and K. Tanamoto. 2006. Structural regions of MD-2 that determine the agonist-antagonist activity of lipid IVa. *J. Biol. Chem.* 281: 5484–5491.
24. Sauter, K. S., M. Brcic, M. Franchini, and T. W. Jungi. 2007. Stable transduction of bovine TLR4 and bovine MD-2 into LPS-nonresponsive cells and soluble CD14 promote the ability to respond to LPS. *Vet. Immunol. Immunopathol.* 118: 92–104.
25. Hobbs, S., S. Jitrapakdee, and J. C. Wallace. 1998. Development of a bicistronic vector driven by the human polypeptide chain elongation factor 1α promoter for creation of stable mammalian cell lines that express very high levels of recombinant proteins. *Biochem. Biophys. Res. Commun.* 252: 368–372.
26. Bryant, C. E., A. Ouellette, K. Lohmann, M. Vandenplas, J. N. Moore, D. J. Maskell, and B. A. Farnfield. 2007. The cellular Toll-like receptor 4 antagonist E5531 can act as an agonist in horse whole blood. *Vet. Immunol. Immunopathol.* 116: 182–189.
27. Derewenda, U., J. Li, Z. Derewenda, Z. Dauter, G. A. Mueller, G. S. Rule, and D. C. Benjamin. 2002. The crystal structure of a major dust mite allergen Der p 2, and its biological implications. *J. Mol. Biol.* 318: 189–197.
28. Shi, J., T. L. Blundell, and K. Mizuguchi. 2001. FUGUE: sequence-structure homology recognition using environment-specific substitution tables and structure-dependent gap penalties. *J Mol Biol.* 310: 243–257.
29. Mizuguchi, K., C. M. Deane, T. L. Blundell, M. S. Johnson, and J. P. Overington. 1998. JOY: protein sequence-structure representation and analysis. *Bioinformatics* 14: 617–623.
30. Sali, A., and T. L. Blundell. 1993. Comparative protein modelling by satisfaction of spatial restraints. *J. Mol. Biol.* 234: 779–815.
31. Binkowski, T. A., S. Naghibzadeh, and J. Liang. 2003. CASTp: computed atlas of surface topography of proteins. *Nucleic Acids Res.* 31: 3352–3355.
32. Katchalski-Katzir, E., I. Shariv, M. Eisenstein, A. A. Friesem, C. Aflalo, and I. A. Vakser. 1992. Molecular surface recognition: determination of geometric fit between proteins and their ligands by correlation techniques. *Proc. Natl. Acad. Sci. USA* 89: 2195–2199.
33. Man-Kuang Cheng, T., T. L. Blundell, and J. Fernandez-Recio. 2007. pyDock: electrostatics and desolvation for effective scoring of rigid-body protein-protein docking. *Proteins* 68: 503–515.
34. Word, J. M., S. C. Lovell, J. S. Richardson, and D. C. Richardson. 1999. Asparagine and glutamine: using hydrogen atom contacts in the choice of side-chain amide orientation. *J. Mol. Biol.* 285: 1735–1747.
35. Gay, N. J., M. Gangloff, and A. N. Weber. 2006. Toll-like receptors as molecular switches. *Nat. Rev. Immunol.* 6: 693–698.
36. Kobayashi, M., S. Saitoh, N. Tanimura, K. Takahashi, K. Kawasaki, M. Nishijima, Y. Fujimoto, K. Fukase, S. Akashi-Takamura, and K. Miyake. 2006. Regulatory roles for MD-2 and TLR4 in ligand-induced receptor clustering. *J. Immunol.* 176: 6211–6218.
37. Wright, C. S., Q. Zhao, and F. Rastinejad. 2003. Structural analysis of lipid complexes of GM2-activator protein. *J. Mol. Biol.* 331: 951–964.
38. Bell, J. K., I. Botos, P. R. Hall, J. Askins, J. Shiloach, D. M. Segal, and D. R. Davies. 2005. The molecular structure of the Toll-like receptor 3 ligand-binding domain. *Proc. Natl. Acad. Sci. USA* 102: 10976–10980.
39. Jin, M. S., S. E. Kim, J. Y. Heo, M. E. Lee, H. M. Kim, S. G. Paik, H. Lee, and J. O. Lee. 2007. Crystal structure of the TLR1-TLR2 heterodimer induced by binding of a tri-acylated lipopeptide. *Cell* 130: 1071–1082.
40. Gangloff, M., A. Murali, J. Xiong, C. J. Arnot, A. N. Weber, A. M. Sandercock, C. V. Robinson, R. Sarisky, A. Holzenburg, C. Kao, and N. J. Gay. 2008. Structural insight into the mechanism of activation of the Toll receptor by the dimeric ligand Spätzle. *J. Biol. Chem.* 283: 14629–14635.